

Quantitative Analysis of ^{11}C -acetate in Nasopharyngeal Carcinoma with Positron Emission Tomography

Yu-Hua Fang* Tsair Kao Liang-Chih Wu¹ Ren-Shyan Liu¹

Institute of Biomedical Engineering, National Yang-Ming University, Taipei, Taiwan, 112, ROC

¹National PET/Cyclotron Center, Taipei Veterans General Hospital, Taipei, Taiwan, 112, ROC

Received 28 Jun 2003; Accepted 14 Aug 2003

Abstract

Although several kinetic models have been proposed for myocardium ^{11}C -acetate PET quantitative studies, currently there are no reports applying them to tumor diagnosis. In this study, we adopted one of the existing models for performing quantitative analysis on nasopharynx carcinoma (NPC) patients. Ten patients were included, with five NPC and five control subjects. For each subject, one ROI of nasopharynx area and one ROI of muscle area were drawn on PET images. Four rate constants were then estimated using the non-linear least squares method. The extraction fraction K was calculated from these estimated parameters. We found K showed significant difference in the two groups, while the average K of nasopharynx areas was 0.2675 ± 0.1562 in NPC and 0.0763 ± 0.0425 in control patients. In addition, a higher ^{11}C -acetate inflow rate constant from plasma was observed in the NPC nasopharynx area, while the clearance rate was lower. Meanwhile, the rate constants of muscle area in the two groups showed no significant difference. These results indicate that, for tumors, those estimated parameters will be significantly different due to the characteristics of ^{11}C -acetate uptake. In conclusion, our results proved the portability of applying kinetic model analysis in ^{11}C -acetate tumor studies. Such an analysis can provide physicians with objective reference for clinical diagnosis.

Keywords: ^{11}C -acetate, PET, Quantitative analysis, Kinetic model

Introduction

Positron emission tomography (PET) has been widely used in clinical diagnosis because of its ability to produce medical functional images. Among the various kinds of tracers in PET, ^{11}C -acetate is one of the most commonly used. Since acetate will be rapidly taken up in tissue and then metabolized to CO_2 via the tricarboxylic acid (TCA) cycle post injection, it is often adopted for cardiac functional evaluation [1-2]. Recent reports suggest that ^{11}C -acetate has also been validated as a useful tracer for tumor detection [3-6]. Abnormally high metabolism of ^{11}C -acetate is observed in regions with possible tumors due to the extreme need of energy through the TCA cycle in tumors.

Although ^{11}C -acetate can be helpful for tumor diagnosis, some diagnostic references are needed in clinical practice because of the poor spatial resolution and limited signal-to-noise ratio of PET images. One diagnostic tool is the quantitative analysis of ^{11}C -acetate PET images. Quantitative analysis manipulates the kinetic models to monitor *in vivo* metabolic activities and obtains physiological parameters

through numerical estimation. Several kinetic models of cardiac ^{11}C -acetate PET have been proposed [7-10]. However, there was no discussion about applying those models in other organs or systems, nor has the ^{11}C -acetate PET quantitative analysis of tumors been developed. Therefore, we attempted in this study to apply one existing kinetic ^{11}C -acetate model to tumors. PET images and data of nasopharyngeal carcinoma (NPC) patients were examined. Physiological parameters were obtained from their data, and further used to compare with those obtained from normal subjects. The aim of this study was to assess whether the chosen model would provide meaningful information from good estimates of physiological parameters for clinical diagnosis.

Materials and Methods

Subjects

Ten subjects were included in this study, five among them with NPC and the other five normal cases acting as controls. All NPC patients were in stage IV according to the JACC 1992 staging system. Disease status was determined by physical examination, bone scan, CT and/or MRI study, clinical follow-up and history. Informed consent was obtained from all patients.

*Corresponding author: Yu-Hua Fang
Tel: +886-2-28267000 ext.5493; Fax: +886-2-28210847
E-mail: dean@bme.ym.edu.tw

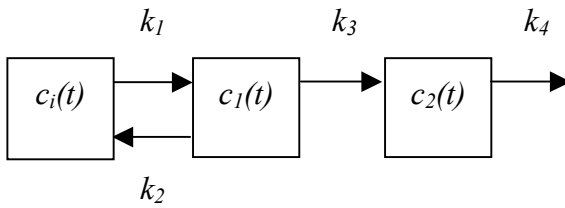


Figure 1. Three-compartment model of ^{11}C -acetate kinetics.

PET procedures

All PET studies were performed in the National PET/Cyclotron Center of Taipei Veterans General Hospital, Taipei, Taiwan with a GE/Scanditronix PC4096-15WB PET scanner. There are eight detector rings in the scanner, producing 15 contiguous slices with thickness of 7 mm per slice and a transaxial resolution of 5.6 mm FWHM in the center. ^{68}Ge was used for attenuation correction before every scan.

After fasting, subjects performing PET scans were intravenously injected with 4.625 Mbq per kg body weight of ^{11}C -acetate. A 15-min dynamic scan was then started immediately post injection, with twelve 10-s, nine 60-s and two 120-s scans. During the PET scan, fifteen arterial or arterialized venous blood samples were taken as the following schedule: 0.2, 0.4, 0.6, 0.8, 1.0, 1.5, 2.0, 2.5, 3.0, 5.0, 7.0, 9.0, 11.0, 13.0, and 15.0 minutes post injection.

^{11}C -acetate kinetic model

As previously mentioned, there have been several ^{11}C -acetate kinetic models proposed for myocardium systems. In this study, we chose the model by Buck et al. [7]. PET images of NPC and control patients were applied on this model to see whether it could be used for quantitative analysis as part of the tumor diagnosis. This model is composed of three compartments, as shown in Figure 1. The first compartment on the left side denotes the input function $c_i(t)$, which is the ^{11}C -acetate plasma time-activity curve (PTAC). From plasma, ^{11}C -acetate enters tissue with the rate constant of k_1 and returns to plasma with rate constant k_2 . $c_1(t)$ denotes the compartment in the middle. Its activities include free acetate and acetyl metabolic intermediates of the TCA cycle. $c_2(t)$ denotes the compartment on the right, being the activity of amino acids that are C-5 glutamine, C-5 glutamate, C-1 glutamine and C-1 glutamate. Since the returning ratio of the amino acids to $c_1(t)$ is very low, there is no rate constant defining the returning rate of amino acids.

According to those relations, the formulation of $c_1(t)$ and $c_2(t)$ can be given as

$$\frac{dc_1(t)}{dt} = k_1 c_i(t) - k_2 c_1(t) - k_3 c_1(t) \quad (1)$$

$$\frac{dc_2(t)}{dt} = k_3 c_1(t) - k_4 c_2(t) \quad (2)$$

Since the tissue time-activity curve from PET image ROI is a composition of two tissue activities, the TTAC $c_t(t)$ can

be defined as

$$c_t(t) = c_1(t) + c_2(t)$$

With Laplace transform, we can find the solution of the above differential equations:

$$c_t(t) = \left(k_1 \left(\frac{k_4 - k_2}{k_4 - k_2 - k_3} \right) \cdot e^{-(k_2 + k_3)t} - \frac{k_1 k_3}{k_4 - k_2 - k_3} \cdot e^{-k_4 t} \right) \otimes c_i(t) \quad (3)$$

Considering the influence of input function on drawn ROIs, a correction term of total blood volume (TBV) is included in the formulation. Defining a ratio constant TBV, among 0 and 1, the real derived TTAC $c_{PET}(t)$ from a ROI will be given as

$$c_{PET}(t) = (1 - TBV) \cdot c_t(t) + TBV \cdot c_i(t) \quad (4)$$

The extraction fraction K , regulated by $k_1 \sim k_3$, is defined as

$$K = \frac{k_1 k_3}{k_2 + k_3}$$

In Buck's study [7], an input function correction for $^{11}\text{CCO}_2$ was performed with simultaneous estimation of related rate constants. To simplify the parameter estimation of this approach, this part of input correction is not included in our study.

Parameter estimation and data analysis

Two ROIs were drawn on each patient's images. The first one was located on the nasopharynx area. For NPC patients, this ROI was drawn according to the location of visually observed tumor area. The second ROI was on the suboccipital muscle. After drawing all these ROIs, the corresponding TTACs were generated from the dynamic PET images. Model analysis was then performed to estimate rate constants $k_1 \sim k_4$ and TBV, using non-linear least squares method (NLLS) for parameter estimation.

The focus of the parameter estimation results was the comparison of K constant between NPC and normal patients. In addition to the comparison of mean values, student's unpaired t-test was conducted on the analysis of K , in order to see whether there was a significant difference ($P < 0.05$) to separate those two groups.

Results

Figure 2 illustrates how the ROIs of nasopharynx and muscle were drawn on images of control and NPC patients. After ROI drawing, generated TTACs were used for parameter estimation. Results for parameter estimation are summarized in Tables 1-2. Table 1 lists the estimation results of the control group. Table 2 shows the results of the NPC group. Units of $k_1 \sim k_4$ and K are min^{-1} . Comparing K of nasopharynx in control

Table 1. Parameter estimation results of control group.

Patient no.	Nasopharynx						Muscle					
	k_1	k_2	k_3	k_4	TBV	K	k_1	k_2	k_3	k_4	TBV	K
1	0.0014	0.0625	0.3457	0.0056	0.0246	0.0357	0.0013	0.2308	0.1457	0.0000	0.0000	0.0147
2	0.0043	0.0912	0.1927	0.0087	0.0298	0.0877	0.0016	0.1809	0.1589	0.0016	0.0000	0.0223
3	0.0054	0.0571	0.3202	0.0081	0.1649	0.1384	0.0028	0.0663	0.3052	0.0086	0.0675	0.0700
4	0.0087	0.1505	0.0697	0.0092	0.0000	0.0824	0.0021	0.1191	0.2014	0.0105	0.0063	0.0402
5	0.0019	0.1715	0.3207	0.0032	0.0739	0.0371	0.0015	0.1980	0.1130	0.0052	0.0000	0.0166
mean	0.0043	0.1066	0.2498	0.0070	0.0586	0.0763	0.0019	0.1590	0.1848	0.0052	0.0148	0.0328
std	0.0029	0.0519	0.1171	0.0025	0.0651	0.0425	0.0006	0.0658	0.0744	0.0045	0.0296	0.0231

Table 2. Parameter estimation results of NPC group.

Patient no.	Nasopharynx						Muscle					
	k_1	k_2	k_3	k_4	TBV	K	k_1	k_2	k_3	k_4	TBV	K
1	0.0067	0.0600	0.2226	0.0060	0.0000	0.1582	0.0020	0.1539	0.1889	0.0118	0.0000	0.0327
2	0.0102	0.0787	0.1923	0.0068	0.1199	0.2166	0.0014	0.1401	0.1847	0.0000	0.0215	0.0245
3	0.0067	0.0022	0.4488	0.0060	0.1038	0.1986	0.0007	0.1756	0.2608	0.0000	0.0000	0.0117
4	0.0181	0.0000	0.2424	0.0136	0.4676	0.5435	0.0027	0.0981	0.2673	0.0177	0.0121	0.0590
5	0.0115	0.0339	0.0609	0.0054	0.1125	0.2208	0.0020	0.0766	0.1559	0.0027	0.0310	0.0396
mean	0.0106	0.0350	0.2334	0.0076	0.1608	0.2675	0.0018	0.1289	0.2115	0.0064	0.0129	0.0335
std	0.0047	0.0348	0.1397	0.0034	0.1784	0.1562	0.0008	0.0407	0.0497	0.0079	0.0136	0.0176

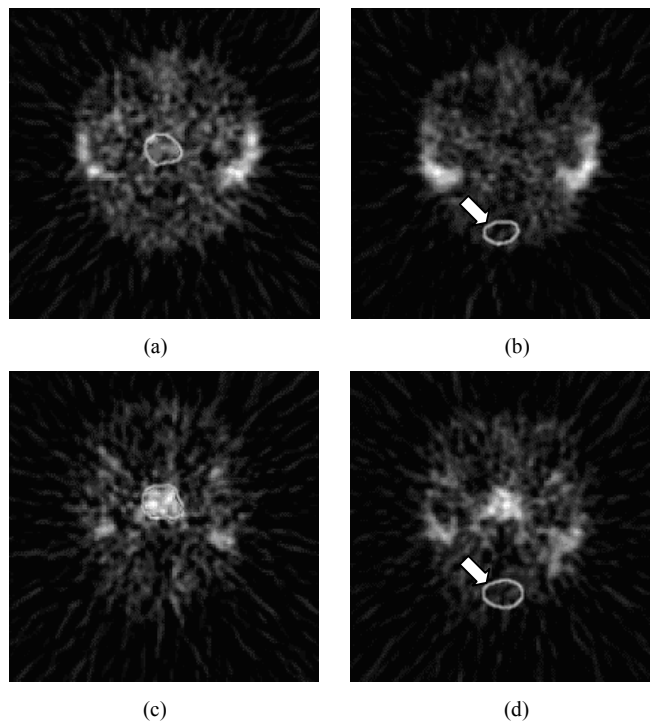


Figure 2. ROI drawing examples. (a) A nasopharynx ROI on one control subject. (b) A muscle ROI on one control subject. (c) A nasopharynx carcinoma ROI on one NPC patient. (d) A muscle ROI on one NPC patient.

and NPC groups, we find that average K was much higher in NPC patients (0.2675 vs. 0.0763). The student's t-test also demonstrated significant difference between K values of

nasopharynx ($P < 0.05$). On the other hand, no significant difference ($P > 0.05$) was observed between K values of muscle in the two groups.

Discussion

Our results indicate that this model could be applied for ^{11}C -acetate quantitative analysis and provide reliable estimates of physiological parameters. From the parameter estimation results, we can first observe that k_1 has quite different tendencies in different types of tissue. First, k_1 is higher in nasopharynx area than in muscle for both groups. But obviously, NPC patients tend to have higher k_1 (0.0106 ± 0.0047 vs. 0.0043 ± 0.0029) in nasopharynx, but similar k_1 in muscle (0.0019 ± 0.0006 vs. 0.0018 ± 0.0008) as compared to the control group. From a physiological point of view, k_1 represents the entrance rate of ^{11}C -acetate and other metabolic intermediates from plasma to tissue. Since tumor tissues usually require abnormally high energy supply, it is reasonable that nasopharynx carcinoma tends to extract a higher ratio of ^{11}C -acetate than normal nasopharynx tissue. On the other hand, k_2 is much higher in normal tissue than in tumors. This can be explained by the fact that tumors have a much lower clearance rate than normal tissue, as reported in Yeh's study [3]. The observation of different k_1 and k_2 tendencies validates that tumors have higher metabolic efficiency for acetate.

As a result of the above facts, it is reasonable that K constant will be significantly different in normal and tumor tissues, since it is proportional to k_1 and k_2^{-1} . In the results, we can find that there is a large difference in K . For tumors, K has a maximum of 0.5435 and a minimum of 0.1582, while in normal nasopharynx, the maximum is only 0.1384 and others are all lower than 0.1. There is no overlap between them. Therefore, K will act as a very good indicator for tumor detection. Since the difference of K in muscle from the two groups is small, high values of K are not induced by the subject variation but by the metabolic activities. Therefore, we can conclude that K can be used as a diagnostic reference for doctors in NPC diagnosis, and perhaps also in other oncology fields.

Compared to [^{18}F]2-fluoro-2-deoxy-D-glucose (FDG), which is also reported as a useful tracer for tumor diagnosis [11, 12], ^{11}C -acetate has several advantages. First, in some organs like the prostate and liver, ^{11}C -acetate has a better sensitivity in tumor detection [4, 6]. Second, shorter scanning time is required in ^{11}C -acetate, as in our study, where only a 15-min dynamic scan was performed. However, FDG has a simple metabolic mechanism, acting merely as energy source for tissue. This fact makes it easier to find FDG's kinetic model. On the other hand, ^{11}C -acetate uptake is more complex, causing its model to be hard to establish. Generally speaking, since ^{11}C -acetate quantitative analysis may act as a faster and more powerful diagnostic tool for tumor diagnosis, more investigation has to be carried out in order to establish a well-accepted kinetic model.

Currently the metabolic mechanisms of ^{11}C -acetate in tumors remain unclear. Compared to the myocardium model, where ^{11}C -acetate is mainly involved in the TCA cycle as source of cardiac energy, only *in vitro* analysis has been reported on this question. In the study of Yoshimoto [5], *in vitro* assessment indicated that abnormally high uptake of

^{11}C -acetate was caused by enhanced lipid synthesis. Our model only reveals physiological conditions of ^{11}C -acetate influx and clearance rates for tissue. We cannot differentiate the individual compound metabolism. Therefore, a future extension of this study could be focused on the development of a kinetic model which is able to separate compartments for different intermediates. Such separation may help toward better explanation of the tumor physiology and provide better diagnostic reference.

Although current investigations upon our chosen model seem to be successful, some improvement of the kinetic model can be worked on. First, the ^{11}C -acetate recirculation correction mentioned in Buck's study [7] was not conducted in our study in order to prevent increasing model complexity. Also, the numerical correction efficiency still remains in doubt. But if we do not consider this issue, the effect of recirculated $^{11}\text{C}\text{CO}_2$ cannot be evaluated and diminished. Second, in the parameter estimation results, TBV did not reveal a meaningful difference between the two groups. However, since abnormal angiogenesis is a common phenomenon in tumors, theoretically we can observe a higher TBV value in tumors. But our results did not show such difference, and the reason is not clear yet. Finally, the quantitative analysis requires a blood sampling procedure to construct the input function. It is invasive and inconvenient. Several methods have been proposed for non-invasive FDG-PET quantitative analysis. The ^{11}C -acetate model also needs a simplified procedure, with fewer blood samples taken, to make this analysis more popular in clinical routine studies. In brief, the above limitations requires more investigation and discussion in order to make the ^{11}C -acetate quantitative analysis portable and helpful for routine tumor diagnosis.

Conclusion

Several findings have been revealed in this study. First, k_1 of tumors is increased because of a higher uptake rate of acetate, a fuel of the TCA cycle for producing energy. Second, k_2 of tumors is decreased as a result of higher metabolic efficiency in tumors. Third, K constant is a good index for NPC diagnosis and possibly other tumors. Further verification of this kinetic model will be achieved, in accordance with our efforts toward developing a more effective model for tumors and more precise parameter estimation in the future.

References

- [1] Porenta G "Noninvasive determination of myocardial blood flow, oxygen consumption and efficiency in normal humans by carbon-11 acetate positron emission tomography imaging," *Eur J Nucl Med* 26:1465-1574, 1999.
- [2] Bengel F. M., Permanetter B., Ungerer M., Nekolla S., Schwaiger M. "Non-invasive estimation of myocardial efficiency using positron emission tomography and carbon-11 acetate – comparison between the normal and failing human heart," *Eur J Nucl Med* 27: 319-326, 2000.
- [3] Yeh S. H., Liu R.S., Wu L.C., Yen S.H., Chang C.W., Chen K.Y. " ^{11}C -acetate clearance in nasopharyngeal carcinoma," *Nucl Med Commun* 20: 131-134, 1999.

- [4] Oyama N., Akino H., Kanamaru H., Suzuki Y., Muamoto S., Yonekura Y., Sadato N., Yamamoto K., Okada K. " ^{11}C -acetate PET imaging of prostate cancer," *J Nucl Med* 43: 181-186, 2002.
- [5] Yoshimoto M., Waki A., Yonekura Y., Sadato N., Omata N., Takahashi N., Welch M. J., Fujibayashi Y. "Characterization of acetate metabolism in tumor cells in relation to cell proliferation: acetate metabolism on tumor cells," *Nucl Med Biol* 28: 117-122, 2001
- [6] Ho C.L., Yu S.C.H., Yeung D.W.C. " ^{11}C -acetate PET imaging in hepatocellular carcinoma and other liver masses," *J Nucl Med* 44: 213-221, 2003.
- [7] Buck A., Wolpers H.G., Hutchins G.D., Savas V., Mangner T.J., Nhuyen N., Schwaiger M. "Effect of carbon-11-acetate recirculation on estimates of myocardial oxygen consumption by PET," *J Nucl Med* 32: 1950-1957, 1991.
- [8] Ng C. K., Huang S.C., Schelbert H.R., Buxton D.B. "Validation of a model for $[1-^{11}\text{C}]$ acetate as a tracer of cardiac oxidative metabolism," *Am J Physiol* 266: H1304-H1315, 1994.
- [9] Sun K. T., Chen K., Huang S.C., Buxton D.B., Hansen H.W., Kim A.S., Siegel S., Choi Y., Muller P., Phelps M.E., Schelbert H.R. "Compartment model for measuring myocardial oxygen consumption using $[1-^{11}\text{C}]$ acetate," *J Nucl Med* 38:459-466, 1997.
- [10] Hoff J., Burchert W., Wolpers H.G., Meyer G.J., Hundeshagen H. "A kinetic model for cardiac PET with $[1-^{11}\text{C}]$ -acetate," *J Nucl Med* 37:521-529, 1996.
- [11] Sadato N., Tsuchida T., Nakaumra S., Waki A., Uematsu H., Takahashi N., Hayashi N., Yonekura Y., Ishii Y. "Non-invasive estimation of the net influx constant using the standardized uptake value for quantification of FDG uptake of tumours," *Eur J Nucl Med* 25: 590-564, 1998.
- [12] Wolfgang A.W., Schwaiger M., Avril N. "Quantitative assessment of tumor metabolism using FDG-PET imaging," *Nucl Med Biol* 27: 683-687, 2000.
-